*Green Energy and Fuel Research (GEFR)*

*Article*

# Microwave Heating Performances of Eucalyptus Camaldulensis Leaves with Silicon Carbide for Biofuel Upgrading

**Faizan Ahmad, Muhammad Kashif, Wenke Zhao and Yaning Zhang ***

School of Energy Science and Engineering, Harbin Institute of Technology, Harbin 150001, China
* Correspondence: ynzhang@hit.edu.cn

Received: 4 December 2024; Revised: 31 December 2024; Accepted: 2 January 2025; Published: 9 January 2025

**Abstract:** Microwave heating is an efficient and effective heating method for upgrading biofuels. This study investigated the heating performance of eucalyptus camaldulensis leaves with and without silicon carbide (SiC) in a microwave chamber. The effects of quartz reactor volume (50, 100, 150, 200, and 250 mL), microwave power (400, 450, 500, 550, and 600 W), and SiC amount (0, 2.5, 5, 7.5, and 10 g) on the heating performance were analyzed. The result showed that as the quartz reactor volume increased from 50 to 250 mL, the average heating rate of eucalyptus leaves without SiC decreased from 153.2 to 47.2 °C/min, while with SiC, it decreased from 366.8 to 106.2 °C/min. As the microwave power increased from 400 to 600 W, the average heating rate of eucalyptus leaves without SiC increased from 73.3 to 197.4 °C/min, and with SiC, it increased from 138.6 to 352.4 °C/min. When SiC amount increased from 0 to 10 g, the average heating rate of eucalyptus leaves increased from 73.9 to 352.4 °C/min. Relationships were proposed to describe the microwave heating performances of eucalyptus camaldulensis leaves with $R^2$ of 0.9953–0.9999.

**Keywords:** heating performance; eucalyptus leave; microwave power; silicon carbide

## 1. Introduction

Fossil fuels have been the primary energy source for over a century, but their limited availability and problems of carbon emissions and global warming pose environmental challenges [1]. The Intergovernmental Panel on Climate Change-IPCC has warned that carbon emissions must be reduced by 50% by 2030 to keep global warming below 1.5 °C [2,3]. Renewable energy sources like solar, wind, and hydroelectric power are crucial for this transition, with biomass energy being one of the most abundant and sustainable options [4]. It holds significant importance due to its numerous benefits, including carbon neutrality, environmental friendliness, affordability, renewability, and versatility [5].

Eucalyptus is the most widely planted tree species in the world, found in over 100 countries and covering more than 20 million hectares of forest. A survey of 95 countries with eucalyptus plantations larger than 5000 hectares estimates that the total area of these plantations worldwide exceeds 22.57 million hectares [6]. Eucalyptus tree is a valuable fuel resource due to its rapid growth, high wood density, favorable chemical properties, low moisture content, and ease of harvesting [7]. Its wood, rich in fiber, is used for firewood, furniture manufacturing, pulp and paper production, and the extraction of essential nutrients and oils [8]. However, the eucalyptus leaves are often discarded as they are not generally consumed by animals. These leaves can degrade soil quality and increase acidity due to the presence of phenolic resin [9]. Waste leaves from eucalyptus trees can be converted into fuels and carbon-based materials through thermochemical techniques including pyrolysis, gasification, carbonization, and liquefaction [10,11]. Among these methods, pyrolysis is especially notable for converting biomass into biogas, bio-oil, and biochar [12]. For the efficient conversion of biomass waste into biofuels, effective heating methods are essential. Microwave heating is an economically viable, homogeneous, and selective heating that offers high energy conversion efficiency [13,14]. As compared with conventional heating, it delivers microwave energy to dielectric materials more effectively, promoting internal heat generation (as shown in Figure 1), enhancing heating rates, and reducing reaction times [15].

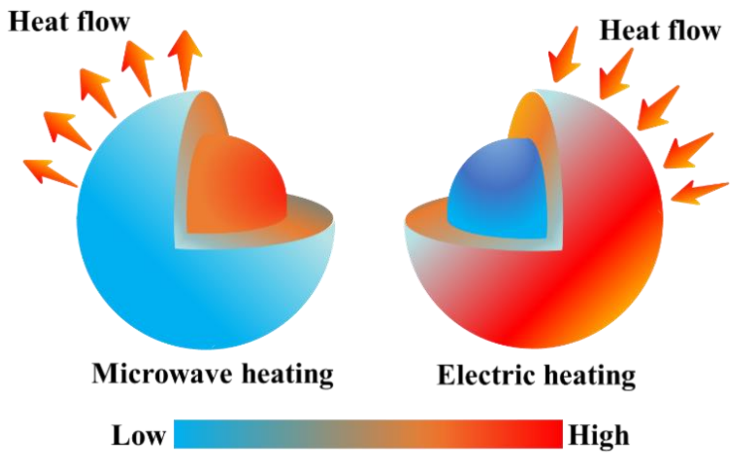


**Figure 1.** Heat transfer mechanism of microwave and electrical heating.

However, due to the poor microwave absorbability of biomass, it cannot reach the desired reaction temperature on its own and requires microwave absorbers as additive. Different microwave absorbers, such as biochar [16,17], graphite [18], metals [19], and silicon carbide (SiC) [20], have been utilized in the microwave-assisted biomass pyrolysis, but SiC is particularly effective due to its chemical resistance, low density, high thermal conductivity, and stability. Fan et al. [21] studied the heating performance of various iron-based microwave absorbers (Fe, $FeS_2$, and $Fe_3O_4$) in comparison to SiC during the pyrolysis process. They achieved a maximum instantaneous heating rate of 209.6 °C/min using SiC as the microwave absorber. Ke et al. [22] investigated the heating absorption characteristics of SiC particles under both conventional and microwave heating. They achieved a heating rate of 7.08 °C/s with microwave heating, which is significantly higher than the 1.95 °C/s rate obtained through conventional heating.

Microwave heating has proven to be an efficient method for biomass pyrolysis and gasification. Moreover, factors such as feeding load, reactor volume, and microwave power significantly influence the efficiency of microwave heating. Singh et al. [23] studied the heating performance of biochar with varying particle sizes (6–8 mm) and feeding loads (25–50 g) at microwave power levels of 400, 700, and 1000 W. Their results showed that increasing the microwave power and feeding load led to increase in the heating rate. Tamang et al. [24] performed a numerical simulation and investigated the effect of microwave power on the heating performance of SiC. The result showed that with increase in microwave power from 300 to 1100 W, the heating rate increased from 20.6 °C/s to 70.8 °C/s. In the study of eucalyptus biomass, Chen et al. [25] performed thermogravimetric analysis of eucalyptus waste at three different heating rates: 5, 10, and 15 °C/min, using a conical-spouted bed reactor to recover bio-oil. They observed that the maximum weight loss occurred at the higher heating rates, indicating a more effective conversion of biomass into bio-oil under these conditions.

Bio-oil produced through the pyrolysis of biomass generally has poor quality due to several factors. Firstly, its chemical composition is complex, containing a mixture of water [26], organic compounds, and various acids, which can lead to instability and challenges in refining. Additionally, the energy density of bio-oil is often lower than that of traditional fossil fuels [27], reducing its effectiveness as an energy source. The presence of corrosive compounds can pose problems for storage and transportation, requiring specialized materials. Furthermore, bio-oil may experience phase separation over time [28], complicating its handling. Its high oxygen content results in reduced heating value and combustion efficiency, while storage stability can be an issue as it may degrade and alter in composition. However, the quality of bio-oil can be improved through upgrading processes, which enhance its properties and make it more suitable for a wider range of applications. Upgrading techniques can include hydrodeoxygenation, where oxygen is removed from the bio-oil, and catalytic cracking, which breaks down larger molecules into smaller, more useful hydrocarbons (aromatic) [29]. These processes help improve the energy density, stability, and combustion efficiency of bio-oil, addressing the quality issues associated with it.

Catalytic cracking has been widely utilized in the upgrading of biofuels, with SiC playing a significant role when coupled or modified with catalysts. SiC is recognized for its high thermal conductivity, chemical stability, and mechanical strength, making it an excellent choice for enhancing catalytic reactions involved in bio-oil upgrading [30,31]. For instance, ZSM-5 zeolite coatings on SiC foam supports have been developed to improve the ex-situ catalytic upgrading of pyrolytic vapors. The high thermal stability and chemical resistance of SiC enhance the efficiency of the biofuel upgrading process, addressing the challenges associated with bio-oil quality [32]. Ou et al. [30] used SiC foam coated with ZSM-5 zeolite for the deoxygenation of anisole and methanol. The results showed the favorable characteristics of SiC foam in the upgrading process, achieving 100% conversion of both anisole and methanol, compared to only 3% conversion with the ZSM-5 catalyst alone. The SiC foam also improved gas-to-solid mass transfer, preventing pore blocking in the catalytic process. In the microwave-assisted pyrolysis of microalgae, da Silveira Rossi et al. [29] used SiC combined with nickel-modified hydrotalcite (NiHTC/SiC) and zeolite (NiHZSM-5/SiC) for bio-oil production. The results indicated that NiHTC/SiC promoted de-nitrification and de-acidification reactions, leading to more alcohols and ketones. Meanwhile, the acid sites of the NiHZSM-5/SiC catalyst further upgraded these compounds into aromatic hydrocarbons. The upgrading values during the pyrolysis process ranged from 17% to 36%. Yu et al. [31] developed a SiC-modified composite catalyst for the hydrothermal treatment of bio-oil. The results demonstrated that this catalyst effectively reduced the oxygenated compounds in the bio-oil while increasing the production of $C_5$–$C_{12}$ hydrocarbons, which primarily fall within the aromatic range.

For upgrading biofuels in the microwave-assisted pyrolysis of eucalyptus camaldulensis leaves, it is essential to first study the heating performance of the leaves with SiC in the microwave chamber. Previous studies have extensively studied pyrolysis [26], gasification [10], thermogravimetric analysis [25], and liquefaction of eucalyptus biomass [33]. However, the comparison of heating performance between eucalyptus leaves with and without a microwave absorber (SiC) in a microwave chamber remains unexplored. This study specifically aimed to: (a) explore the heating performances of eucalyptus camaldulensis leaves under microwave irradiation, both with and without SiC; (b) investigate the effects of quartz reactor volume, microwave power, and feeding load of SiC on the heating performance of eucalyptus leaves, both individually and in combination with SiC; and (c) develop equations to estimate the transient temperatures for eucalyptus leaves.

## 2. Experimental

### *2.1. Feedstock*

In this study, eucalyptus leaves were sourced from Eucalyptus camaldulensis trees in Pakistan. The leaves were dried naturally by being left in the open air at temperatures between 39 and 41 °C. The leaves underwent a natural drying technique, where they were exposed to ambient air temperatures ranging from 39 to 41 °C for natural drying. After this initial drying, the leaves were washed with water to remove dust and impurities and then further dried in an oven at 80 °C for one day. Once dried, the leaves were ground and sieved through a 60-mesh screener to achieve a particle size of 0.25 mm. The final preparation of the experimental material is shown in Figure 2. The proximate and ultimate analyses of the eucalyptus leaves are detailed in Table 1. SiC particles with 99.90% purity and sizes ranging from 1–2 mm were utilized as microwave absorber during this study.


**Figure 2.** Final preparation of the experimental material.

**Table 1.** Proximate and ultimate analysis of eucalyptus leaves.

| **Proximate Analysis (wt.%)** | | | | **Ultimate Analysis (wt.%)** | | | | |
|---|---|---|---|---|---|---|---|---|
| $M_{ad}$ | $A_{ad}$ | $V_{ad}$ | $FC^a$ | S | N | H | $O^a$ | C |
| 3.32 | 4.62 | 77.21 | 14.85 | 0.16 | 1.86 | 6.43 | 44.99 | 46.56 |

Note: $_{ad}$ for air drying basis; $^a$ calculated by differential subtraction. M, A, V and FC are moisture contents, ash contents, volatile contents and fixed carbon.

### *2.2. Experimental Process*

The experimental setup for conducting the heating performance of eucalyptus leaves is shown in Figure 3 and includes: (1) microwave oven, (2) quartz reactor, (3) digital thermometer, (4) K-type thermocouple, (5) connecting tube, (6) vacuum pump, and (7) electric power meter. The microwave oven served as the main heating source, with adjustable microwave power levels ranging from 0 to 100 W and operating at a frequency of 2450 MHz. Its cavity dimensions were 300 × 300 × 350 mm$^3$. The K-type thermocouple was used to measure the temperature of the feedstock inside the quartz reactor, and the readings were displayed on the digital thermometer. This thermocouple can measure temperatures up to 1000 °C with uncertainty of ±0.1 °C. Additionally, a power meter monitored the electricity consumption of the microwave oven.

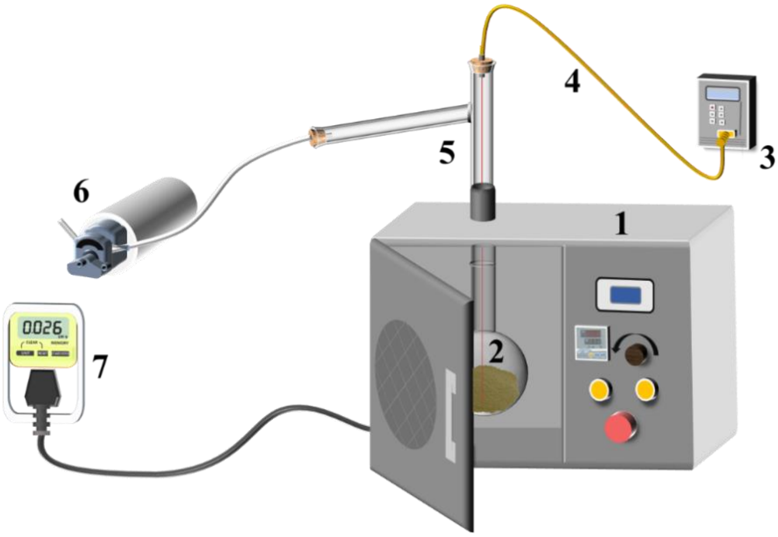


**Figure 3.** Experimental setup of microwave heating performance, 1—microwave oven, 2—quartz reactor, 3—digital thermometer, 4—K-type thermocouple, 5—connecting tube, 6—vacuum pump, 7—electric power meter.

For the heating performance experiments, 10 g of eucalyptus leaves and a specified amount of SiC particles (0–10 g) were carefully weighed and mixed homogeneously. This mixture was then placed in the quartz reactor, which was positioned inside the microwave oven. To minimize heat dissipation, the microwave oven cavity was filled with cotton wool. The vacuum pump was activated for 5–7 min to achieve inert environment within the quartz reactor. The microwave oven was set to the desired power level (400–600 W), and the experiment started by turning on the microwave oven. The design of the experiments is presented in Table 2.

After turning on the microwave oven, the initial temperature of the feedstock was recorded. The temperature was then measured at regular intervals of 10 s. The experiments concluded once the feedstock reached 200 °C, and each experiment was repeated twice. The average heating rate of the eucalyptus leaves and the mixture of eucalyptus leaves and SiC particles can be determined using Equation (1).

$$H = \frac{T_2 - T_1}{t_o} \tag{1}$$

where $H$ denotes the average heating rate (°C/min), $T_2$ denotes the final temperature (°C), $T_1$ denotes the initial temperature (°C), and $t_o$ denotes the time of microwave heating (min).

**Table 2.** Experimental design for heating performance.

| No. | Reactor Volume (mL) | Microwave Power (W) | SiC Amount (g) | Eucalyptus Amount (g) |
|---|---|---|---|---|
| 1 | 50 | 400 | 0 | 10 |
| 2 | 50 | 400 | 10 | 10 |
| 3 | 100 | 400 | 0 | 10 |
| 4 | 100 | 400 | 10 | 10 |
| 5 | 150 | 400 | 0 | 10 |
| 6 | 150 | 400 | 10 | 10 |
| 7 | 200 | 400 | 0 | 10 |
| 8 | 200 | 400 | 10 | 10 |
| 9 | 250 | 400 | 0 | 10 |
| 10 | 250 | 400 | 10 | 10 |
| 11 | 100 | 450 | 0 | 10 |
| 12 | 100 | 450 | 10 | 10 |
| 13 | 100 | 500 | 0 | 10 |
| 14 | 100 | 500 | 10 | 10 |
| 15 | 100 | 550 | 0 | 10 |
| 16 | 100 | 550 | 10 | 10 |
| 17 | 100 | 600 | 0 | 10 |
| 18 | 100 | 600 | 10 | 10 |
| 19 | 100 | 400 | 2.5 | 10 |
| 20 | 100 | 400 | 5 | 10 |
| 21 | 100 | 400 | 7.5 | 10 |

## 3. Results and Discussion

### *3.1. Effect of Quartz Reactor Volume*

The effect of quartz reactor volume on the heating performance of eucalyptus leaves, both with and without SiC, is shown in Figure 4. Throughout the investigation, microwave power, the amount of eucalyptus leaves, and SiC were kept constant at 400 W, 10 g, and (0 g, 10 g), respectively. For reactor volumes of 50, 100, 150, 200, and 250 mL, the average heating rates of eucalyptus leaves without SiC were recorded as 153.2, 73.3, 67.2, 61.8, and 47.2 °C/min, respectively. The heating durations for eucalyptus leaves to reach temperatures of 201.7, 200.8, 201.9, 203.6, and 200.4 °C were 72, 141, 156, 168, and 219 s, respectively. In contrast, with 10 g of SiC, the average heating rates were higher, indicating 366.8, 179.6, 155.1, 137.7, and 106.2 °C/min, respectively, for the same reactor volumes. The corresponding heating times to reach temperatures of 205.4, 202.3, 203.5, 202.5, and 202.5 °C were 30, 61, 70, 79, and 101 s, respectively.

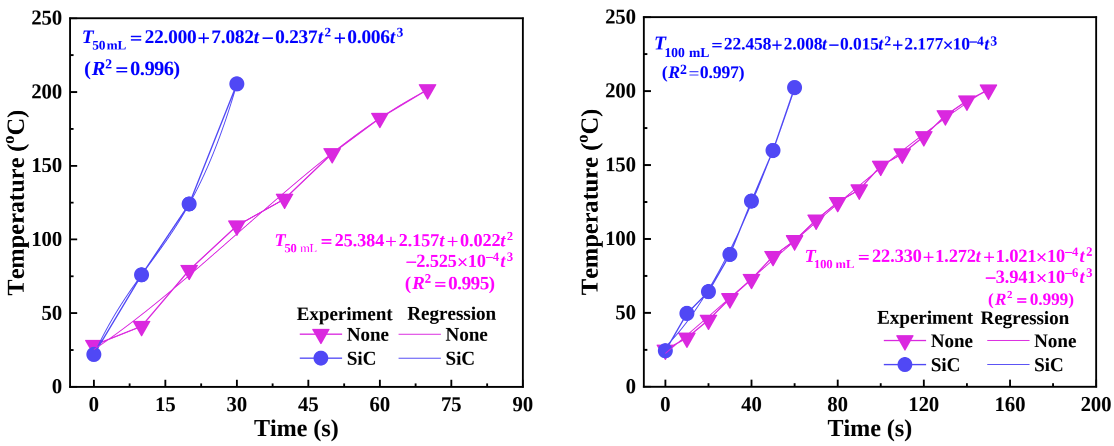


(**a**) 50 mL (**b**) 100 mL

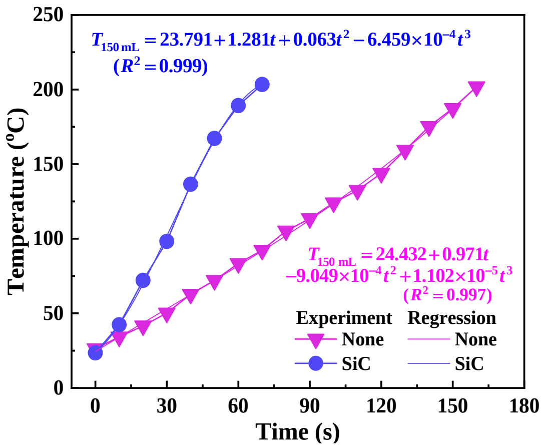


(**c**) 150 mL

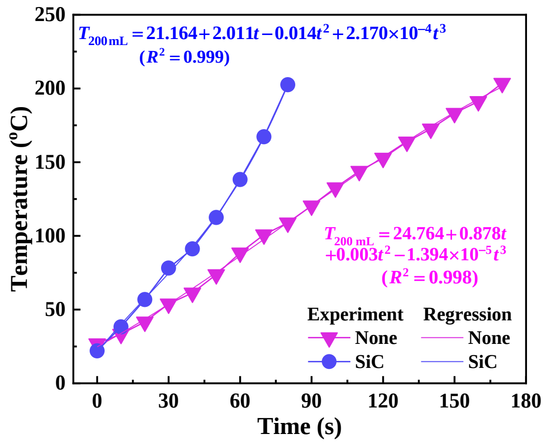


(**d**) 200 mL

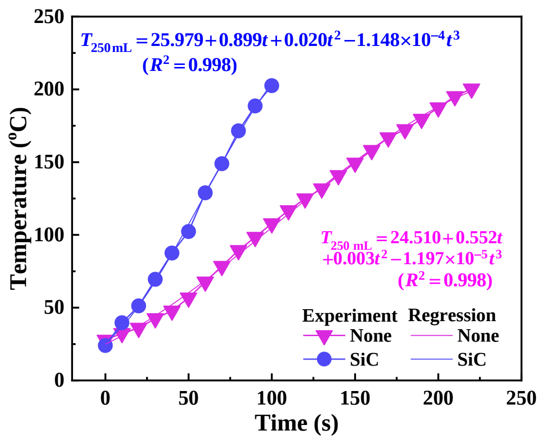


(**e**) 250 mL

**Figure 4.** Recorded and approximated temperatures of eucalyptus leaves with/without SiC at different quartz reactor volumes, (**a**) 50 mL, (**b**) 100 mL, (**c**) 150 mL, (**d**) 200 mL, and (**e**) 250 mL.

With the increase in quartz reactor volume, the heating rates of eucalyptus leaves without SiC decreased from 153.2 °C/min to 47.2 °C/min and with SiC it decreased from 366.8 °C/min to 47.2 °C/min as shown in Figure 4. The decrease in the heating rate with increase in quartz reactor volume can be attributed to the increase in the heat loss area per unit mass of the feedstock resulting from the larger reactor volume [26]. Additionally, larger reactors may experience greater heat loss to the environment and altered heating kinetics, leading to less efficient heating. The observed decrease in heating rate with increase in quartz reactor volume is consistent with the results in the study [22]. However, the addition of SiC results in a steeper slope of the heating curve (Figure 4), showing a more rapid increase in temperature over time. This suggests that the heating process becomes more efficient, and the temperature of the eucalyptus leaves rises more quickly compared to when SiC was not present [34]. The excellent thermal conductivity of SiC, as a high-performance ceramic material, is responsible for this enhancement in heating efficiency [35].

The regression fitting equations for the temperatures of eucalyptus leaves without SiC at different quartz reactor volumes, are obtained as follows:

$$T_{50\text{ mL}} = 25.384 + 2.157t + 0.022t^2 - 2.525\times10^{-4}t^3 \quad (\mathrm{R}^2 = 0.995) \tag{2}$$

$$T_{100\text{ mL}} = 22.330 + 1.272t + 1.021t^2 - 3.941\times10^{-7}t^3 \quad (\mathrm{R}^2 = 0.999) \tag{3}$$

$$T_{150\text{ mL}} = 24.432 + 0.971t - 9.049\times10^{-4}t^2 + 1.102\times10^{-5}t^3 \quad (\mathrm{R}^2 = 0.997) \tag{4}$$

$$T_{200\text{ mL}} = 24.764 + 0.878t + 0.003t^2 - 1.394\times10^{-5}t^3 \quad (\mathrm{R}^2 = 0.998) \tag{5}$$

$$T_{250\text{ mL}} = 24.510 + 0.552t + 0.003t^2 - 1.197\times10^{-5}t^3 \quad (\mathrm{R}^2 = 0.998) \tag{6}$$

With 10 g of SiC, the regression fitting equations are as follows:

$$T_{50\ \mathrm{mL}} = 22.000 + 7.082t - 0.237t^2 + 0.006t^3 \quad (\mathrm{R}^2 = 0.996) \tag{7}$$

$$T_{100\ \mathrm{mL}} = 22.458 + 2.008t + 0.015t^2 + 2.177 \times 10^{-4} t^3 \quad (\mathrm{R}^2 = 0.997) \tag{8}$$

$$T_{150\ \mathrm{mL}} = 23.791 + 1.281t + 0.063t^2 - 6.459 \times 10^{-4} t^3 \quad (\mathrm{R}^2 = 0.999) \tag{9}$$

$$T_{200\ \mathrm{mL}} = 21.164 + 2.011t - 0.014t^2 + 2.170 \times 10^{-4} t^3 \quad (\mathrm{R}^2 = 0.999) \tag{10}$$

$$T_{250\ \mathrm{mL}} = 25.979 + 0.899t + 0.020t^2 - 1.148 \times 10^{-4} t^3 \quad (\mathrm{R}^2 = 0.998) \tag{11}$$

where $T$ denotes the temperature within 200 °C, $t$ denotes the time in seconds, and $\mathrm{R}^2$ denotes the coefficient of determination.

The heating time is the main factor influencing the temperature of eucalyptus leaves alone and with SiC during microwave heating. For the quartz reactor volumes of 50, 100, 150, 200, and 250 mL, the recorded temperatures of eucalyptus leaves can be estimated using the following equations: Equation (2) for the heating time range $0 \le t \le 72$ s, Equation (3) for $0 \le t \le 141$ s, Equation (4) for $0 \le t \le 156$ s, Equation (5) for $0 \le t \le 168$ s, and Equation (6) for $0 \le t \le 219$ s. Similarly, for the combination of eucalyptus leaves and SiC, the recorded temperatures can be estimated using equations: Equation (7) for the heating time range $0 \le t \le 30$ s, Equation (8) for $0 \le t \le 61$ s, Equation (9) for $0 \le t \le 70$ s, Equation (10) for $0 \le t \le 79$ s, and Equation (11) for $0 \le t \le 101$ s.

### *3.2. Effect of Microwave Power*

The effects of microwave power on the heating performances of eucalyptus leaves with and without SiC are shown in Figure 5. Throughout the investigation, quartz reactor volume, the amount of eucalyptus leaves, and SiC were kept constant at 100 mL, 10 g, and (0 g, 10 g), respectively. Under microwave power levels of 400, 450, 500, 550, and 600 W, the average heating rates of eucalyptus leaves without SiC were 73.3, 87.4, 96.4, 119.3, and 197.4 °C/min. The heating durations for eucalyptus leaves to reach temperatures of 200.8, 201.6, 202.3, 200.7, and 200.2 °C were 141, 118, 107, 87, and 52 s, respectively. In contrast, when 10 g of SiC was added, the average heating rates were notably higher across all power levels. The heating rates were 138.6, 185.6, 219.5, 266.3, and 352.4 °C/min, respectively. The corresponding heating times to reach temperatures of 202.3, 201.7, 200.8, 203.1, and 200.2 °C were 61, 58, 49, 41, and 30 s, respectively. With increase in microwave power, the average heating rate of eucalyptus leaves without SiC increased significantly from 73.3 °C/min to 197.4 °C/min. When 10 g of SiC was added, the average heating rate improved even further, increasing from 138.6 °C/min to 352.4 °C/min. This increase in heating rate can be attributed to the enhanced energy density, which allows for greater absorption of energy by the feedstock [20,36]. At higher microwave power levels, more microwaves are available, leading to increased molecular agitation and more efficient heating [37]. The maximum average heating rate of 352.4 °C/min was observed at 600 W with SiC particles, where the heating curve is notably steeper (Figure 5e), indicating a rapid temperature increase.

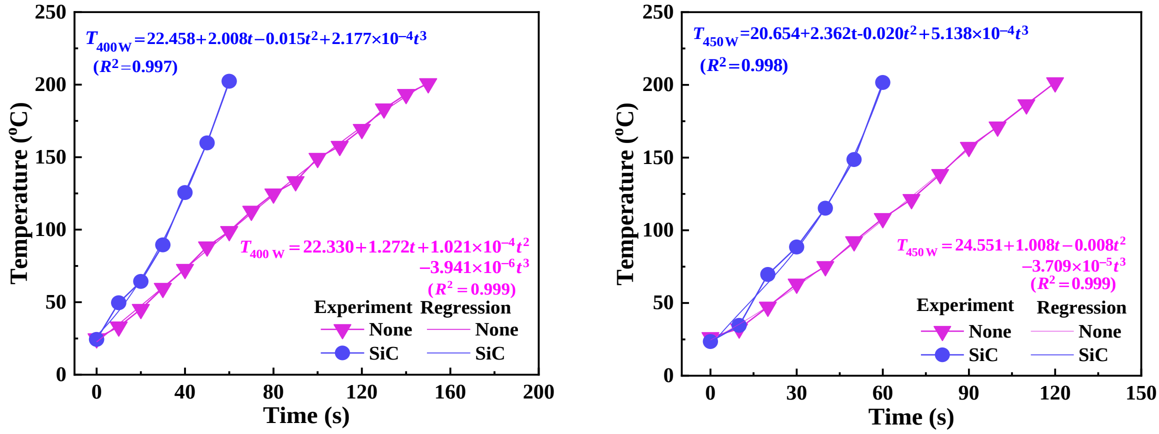


(**a**) 400 W

(**b**) 450 W

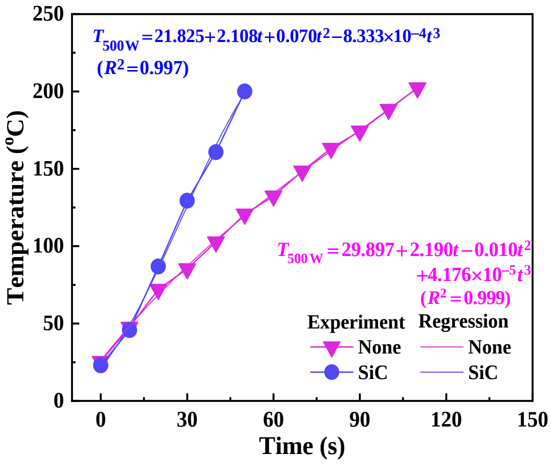


(**c**) 500 W

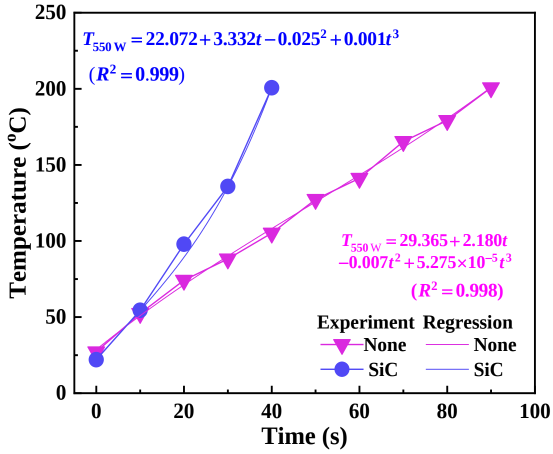


(**d**) 550 W

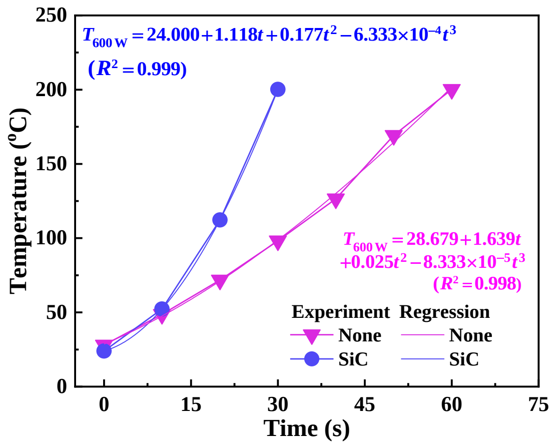


(**e**) 600 W

**Figure 5.** Recorded and approximated temperatures of eucalyptus leaves with/without SiC at different microwave powers, (**a**) 50 mL, (**b**) 100 mL, (**c**) 150 mL, (**d**) 200 mL, and (**e**) 250 mL.

The regression fitting equations for the temperatures of eucalyptus leaves without SiC at various microwave powers are obtained as follows:

$$T_{400\ \mathrm{W}} = 22.330 + 1.272t + 1.021\times10^{-4}t^2 - 3.941\times10^{-6}t^3 \quad (\mathrm{R}^2 = 0.999) \tag{12}$$

$$T_{450\ \mathrm{W}} = 24.551 + 1.008t - 0.008t^2 - 3.709\times10^{-5}t^3 \quad (\mathrm{R}^2 = 0.999) \tag{13}$$

$$T_{500\ \mathrm{W}} = 29.897 + 2.190t - 0.010t^2 + 4.176\times10^{-5}t^3 \quad (\mathrm{R}^2 = 0.999) \tag{14}$$

$$T_{550\ \mathrm{W}} = 29.365 + 2.180t - 0.007t^2 + 5.275\times10^{-5}t^3 \quad (\mathrm{R}^2 = 0.998) \tag{15}$$

$$T_{600\ \mathrm{W}} = 28.678 + 1.639t + 0.025t^2 - 8.333\times10^{-5}t^3 \quad (\mathrm{R}^2 = 0.998) \tag{16}$$

With 10 g of SiC the regression fitting equations are as follows:

$$T_{400\ \mathrm{W}} = 22.458 + 2.008t + 0.015t^2 - 2.177\times10^{-4}t^3 \quad (\mathrm{R}^2 = 0.997) \tag{17}$$

$$T_{450\ \mathrm{W}} = 20.654 + 2.362t - 0.020t^2 - 5.138\times10^{-4}t^3 \quad (\mathrm{R}^2 = 0.998) \tag{18}$$

$$T_{500\ \mathrm{W}} = 21.825 + 2.108t - 0.070t^2 + 8.333\times10^{-4}t^3 \quad (\mathrm{R}^2 = 0.997) \tag{19}$$

$$T_{550\ \mathrm{W}} = 22.072 + 3.332t - 0.0252t^2 + 0.001t^3 \quad (\mathrm{R}^2 = 0.999) \tag{20}$$

$$T_{600\ \mathrm{W}} = 24.000 + 1.118t + 0.177t^2 - 6.333\times10^{-4}t^3 \quad (\mathrm{R}^2 = 0.999) \tag{21}$$

The temperature of the eucalyptus leaves with and without SiC is mainly influenced by the heating time. For the microwave power 400, 450, 500, 550, and 600 W, the recorded temperatures of eucalyptus leaves can be estimated using the following equations: Equation (12) for the heating time range $0 \le t \le 141$ s, Equation (13) for $0 \le t \le 118$ s, Equation (14) for $0 \le t \le 107$ s, Equation (15) for $0 \le t \le 87$ s, and Equation (16) for $0 \le t \le 52$ s. Similarly, for the combination of eucalyptus leaves and SiC, the recorded temperatures can be estimated using equations: Equation (17) for the heating time range $0 \le t \le 61$ s, Equation (18) for $0 \le t \le 58$ s, Equation (19) for $0 \le t \le 49$ s, Equation (20) for $0 \le t \le 41$ s, and Equation (21) for $0 \le t \le 30$ s.

### *3.3. Effect of SiC Amount*

The effect of different SiC (0, 2.5, 5, 7.5, and 10 g) on heating performance of eucalyptus leaves is shown in Figure 6. Throughout the investigation, the microwave power, amount of eucalyptus leaves, and quartz reactor volume were constant at 600 W, 10 g, and 100 mL. With the SiC amount of 0, 2.5, 5, 7.5, and 10 g, the average heating rates were 73.9, 99.6, 138.9, 193.2, and 352.4 °C/min. The time required to reach temperatures of 200.8, 203.5, 206.4, 204.3, and 200.2 °C was of 141, 109, 79, 60, and 30 s, respectively. With increase in the amount of SiC, the average heating rate of eucalyptus leaves increased due to the higher concentration of SiC particles in the feedstock. More SiC particles enhance microwave absorption, which is dissipated as heat, promoting greater molecular agitation and faster heating [38]. Additionally, the increased concentration of SiC provides a larger surface area for absorption, improving the dielectric properties and facilitating a more efficient heating process [39].

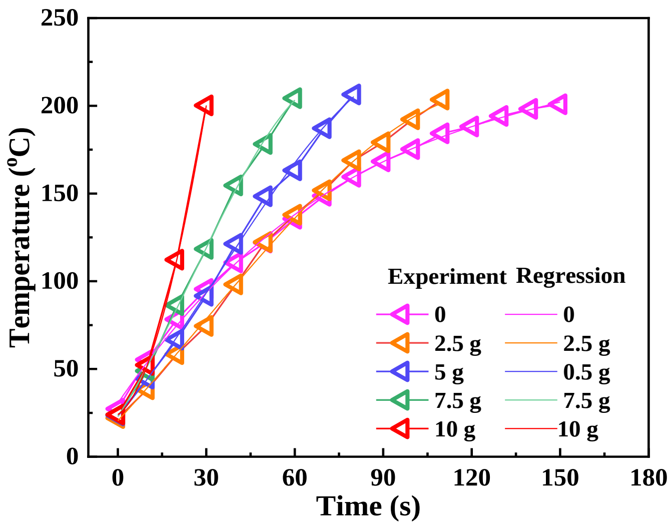


**Figure 6.** Recorded and approximated temperatures of eucalyptus leaves at different amount of SiC.

During the process of microwave heating, the temperature of the eucalyptus leaves is affected by the heating time. For the SiC amount of 0, 2.5, 0.5, 0.75, and 10 g, the transient temperatures can be estimated using the following equations: Equation (22) for the heating time range $0 \le t \le 141$ s, Equation (23) for $0 \le t \le 109$ s, Equation (24) for $0 \le t \le 79$ s, Equation (25) for $0 \le t \le 60$ s, and Equation (26) for $0 \le t \le 30$ s.

$$T_0 = 30.530 + 2.455t - 0.012t^2 + 2.592\times10^{-5}t^3 \quad (\mathrm{R}^2 = 0.999) \tag{22}$$

$$T_{2.5\ \mathrm{g}} = 20.481 + 1.831t + 0.005t^2 - 6.430\times10^{-5}t^3 \quad (\mathrm{R}^2 = 0.998) \tag{23}$$

$$T_{5\ \mathrm{g}} = 22.993 + 1.979t + 0.017t^2 - 1.709\times10^{-4}t^3 \quad (\mathrm{R}^2 = 0.996) \tag{24}$$

$$T_{7.5\ \mathrm{g}} = 23.019 + 2.536t + 0.036t^2 - 4.777\times10^{-4}t^3 \quad (\mathrm{R}^2 = 0.998) \tag{25}$$

$$T_{10\ \mathrm{g}} = 24.000 + 1.118t + 0.177t^2 - 6.333\times10^{-4}t^3 \quad (\mathrm{R}^2 = 0.999) \tag{26}$$

The $R^2$ values obtained from the calculation of regression statistics are within the range of [0, 1]. The closer the value is to 1, the stronger the ability of the dependent variable of the regression equation to the microwave heating temperature of eucalyptus leaves and the better fitting effect of this regression equation. Similarly, the higher the value, the smaller the difference from $R^2$, indicating greater accuracy of the regression equation. The $R^2$ regression values show that Equations (22) to (26) are effective in estimating the transient temperatures of eucalyptus leaves at different amounts of SiC loading.

## 4. Conclusions

This study investigated the microwave heating performance of eucalyptus camaldulensis leaves, both with and without silicon carbide. The effects of quartz reactor volume, microwave power, and SiC amount on heating performance were studied. As the quartz reactor volume increased from 50 to 250 mL, the average heating rate of eucalyptus leaves without SiC decreased from 153.2 to 47.2 °C/min, while with 10 g of SiC, it decreased from 366.8 to 106.2 °C/min. Conversely, as microwave power increased from 400 to 600 W, the average heating rate of eucalyptus leaves without SiC increased from 73.3 to 197.4 °C/min, and with 10 g of SiC, it increased from 138.6 to 352.4 °C/min. However, as the amount of SiC increased from 0 to 10 g, the heating rate improved from 73.9 to 352.4 °C/min. The optimal heating rate of 366.8 °C/min was achieved in 50 mL quartz reactor using 10 g SiC at 400 W. Equations were proposed to estimate the temperatures, and the $R^2$ values for the effects of quartz reactor volume, microwave power, and SiC amount were in the ranges of 0.995–0.999, 0.997–0.998, and 0.997–0.998, respectively. These results show that the incorporation of SiC significantly enhanced the heating rate of eucalyptus camaldulensis leaves, which is essential for optimizing biofuel upgrading processes in future research.

**Author Contributions:** Faizan Ahmad: writing—original draft preparation; Muhammad Kashif: investigation; Wenke Zhao: validation; Yaning Zhang: supervision. All authors have read and agreed to the published version of the manuscript.

**Funding:** Financial support was provided by the National Natural Science Foundation of China (52076049, 52476005), Heilongjiang Province "Double First-class" Discipline Collaborative Innovation Achievement Project (Grant No. LJGXCG2023-080), Heilongjiang Provincial Key R&D Program (Grant No. 2023ZX02C05), and Heilongjiang Provincial Key R&D Program "Unveiling the Leader" Project (Grant No. 2023ZXJ02C04).

**Institutional Review Board Statement:** Not applicable.

**Informed Consent Statement:** Not applicable.

**Data Availability Statement:** Data will be made available on request.

**Conflicts of Interest:** The authors declare no conflict of interest.

## References

1. Chen, W.H. Progress in Green Energy and Fuel for Sustainability. *Green Energy Fuel Res.* **2024**, *1*, 13–22.
2. Hoegh-Guldberg, O.; Jacob, D.; Taylor, M.; et al. The human imperative of stabilizing global climate change at 1.5 °C. *Science* **2019**, *365*, eaaw6974.
3. Lee, J.; Im, G.; Yoo, J.H.; et al. Development of greenhouse gas ($CO_2$) emission factor for Korean coal briquettes. *Energy Sources Part A Recovery Util. Environ. Eff.* **2015**, *37*, 1415–1423.
4. Zhang, C.; Fang, J.; Zhan, Y.; et al. Life Cycle Assessment of Microalgal Carbon Fixation and Torrefaction for Carbon Neutralization: A State-of-the-Art Review. *Green Energy Fuel Res.* **2024**, *1*, 23–38.
5. Wu, H.; Lyu, Y.; Wang, R.; et al. Power Generation Enhancement in a Solar Energy and Biomass-Based Distributed Energy System using $H_2O/CO_2$ Hybrid Gasification. *J. Therm. Sci.* **2024**, *33*, 1657–1671.
6. Zhang, Y.; Wang, X. Geographical spatial distribution and productivity dynamic change of eucalyptus plantations in China. *Sci. Rep.* **2021**, *11*, 19764.
7. Penín, L.; López, M.; Santos, V.; et al. Technologies for Eucalyptus wood processing in the scope of biorefineries: A comprehensive review. *Bioresour. Technol.* **2020**, *311*, 123528.
8. Seng Hua, L.; Wei Chen, L.; Antov, P.; et al. Engineering wood products from *Eucalyptus* spp. *Adv. Mater. Sci. Eng.* **2022**, *1*, 8000780.
9. Kabir, M.G.; Wang, Y.; Abuhena, M.; et al. A bio-sustainable approach for reducing Eucalyptus tree-caused agricultural ecosystem hazards employing Trichoderma bio-sustained spores and mycorrhizal networks. *Front. Microbiol.* **2023**, *13*, 1071392.
10. Louw, J.; Schwarz, C.E.; Burger, A.J. Supercritical water gasification of eucalyptus grandis and related pyrolysis char: Effect of feedstock composition. *Bioresour. Technol.* **2019**, *216*, 1030–1039.

11. Kosanić, T.R.; Ćeranić, M.B.; Đurić, S.N.; et al. Experimental investigation of pyrolysis process of woody biomass mixture. *J. Therm. Sci.* **2014**, *23*, 290–296.
12. Zhang, X.; Yang, X.; Yuan, X.; et al. Effect of pyrolysis temperature on composition, carbon fraction and abiotic stability of straw biochars: Correlation and quantitative analysis. *Carbon Res.* **2022**, *1*, 17.
13. Zhang, Y.; Hong, X.; Shen, X.; et al. Heavy oil catalytic upgrading with microwave heating over a microwave absorbing catalyst USY/AC/$Al_2O_3$. *Energy Sources Part A Recovery Util. Environ. Eff.* **2019**, *41*, 229–236.
14. Kostas, E.T.; Beneroso, D.; Robinson, J.P. The application of microwave heating in bioenergy: A review on the microwave pre-treatment and upgrading technologies for biomass. *Renew. Sustain. Energy Rev.* **2017**, *77*, 12–27.
15. Ho, S.H.; Zhang, C.; Chen, W.H.; et al. Characterization of biomass waste torrefaction under conventional and microwave heating. *Bioresour. Technol.* **2018**, *264*, 7–16.
16. Sakhiya, A.K.; Anand, A.; Kaushal, P. Production, activation, and applications of biochar in recent times. *Biochar* **2020**, *2*, 253–285.
17. Ren, J.; Jiang, J.; Wang, J.; et al. Variable frequency microwave induced $CO_2$ Boudouard reaction over biochar. *Biochar* **2024**, *6*, 20.
18. Peymanfar, R.; Ershad, Z.S.; Selseleh-Zakerin, E.; et al. Graphite-like carbon nitride (g-$C_3N_4$): A promising microwave absorber. *Ceram. Int.* **2022**, *48*, 16461–16476.
19. Li, L.; Ma, X.; Xu, Q.; et al. Influence of microwave power, metal oxides and metal salts on the pyrolysis of algae. *Bioresour. Technol.* **2013**, *142*, 469–474.
20. Chen, G.; Li, J.; Cheng, Z.; et al. Investigation on model compound of biomass gasification tar cracking in microwave furnace: Comparative research. *Appl. Energy* **2018**, *217*, 249–257.
21. Fan, S.; Zhang, Y.; Cui, L.; et al. Conversion of polystyrene plastic into aviation fuel through microwave-assisted pyrolysis as affected by iron-based microwave absorbents. *ACS Sustain. Chem. Eng.* **2023**, *11*, 1054–1066.
22. Ke, C.; Liu, T.; Zhang, Y.; et al. Energy absorption performances of silicon carbide particles during microwave heating process. *Chem. Eng. Process.-Process Intensif.* **2022**, *172*, 108796.
23. Singh, R.; Lindenberger, C.; Chawade, A.; et al. Unveiling the microwave heating performance of biochar as microwave absorber for microwave-assisted pyrolysis technology. *Sci. Rep.* **2024**, *14*, 9222.
24. Tamang, S.; Aravindan, S. 3D numerical modelling of microwave heating of SiC susceptor. *Appl. Therm. Eng.* **2019**, *162*, 114250.
25. Chen, Z.; Zhu, Q.; Wang, X.; et al. Pyrolysis behaviors and kinetic studies on eucalyptus residues using thermogravimetric analysis. *Energy Convers. Manag.* **2015**, *105*, 251–259.
26. Amutio, M.; Lopez, G.; Alvarez, J.; et al. Fast pyrolysis of eucalyptus waste in a conical spouted bed reactor. *Bioresour. Technol.* **2015**, *194*, 225–232.
27. Sánchez-Borrego, F.J.; Alvarez-Mateos, P.; Garcia-Martin, J.F. Biodiesel and other value-added products from bio-oil obtained from agrifood waste. *Processes* **2021**, *9*, 797.
28. Han, Y.; Paiva Pinheiro Pires, A.; Denson, M.; et al. Ternary phase diagram of water/bio-oil/organic solvent for bio-oil fractionation. *Energy Fuels* **2020**, *34*, 16250–16264.
29. da Silveira Rossi, R.A.; Dai, L.; de Souza Barrozo, M.A.; et al. Bio-fuel production from catalytic microwave-assisted pyrolysis of the microalgae *Schizochytrium limacinum* in a tandem catalytic bed. *Chem. Eng. J.* **2023**, *478*, 147223.
30. Ou, X.; Wu, C.; Shi, K.; et al. Structured ZSM-5/SiC foam catalysts for bio-oils upgrading. *Appl. Catal. A Gen.* **2020**, *599*, 117626.
31. Yu, Z.; Wang, Y.; Jiang, L.; et al. Conversion of woody oil into bio-oil in a downdraft reactor using a novel silicon carbide foam supported MCM41 composite catalyst. *RSC Adv.* **2019**, *9*, 19729–19739.
32. Tuci, G.; Liu, Y.; Rossin, A.; et al. Porous silicon carbide (SiC): A chance for improving catalysts or just another active-phase carrier? *Chem. Rev.* **2021**, *121*, 10559–10665.
33. Seehar, T.H.; Toor, S.S.; Sharma, K.; et al. Influence of process conditions on hydrothermal liquefaction of eucalyptus biomass for biocrude production and investigation of the inorganics distribution. *Sustain. Energy Fuels* **2021**, *5*, 1477–1487.
34. Cui, L.; Qin, N.; Li, H.; et al. Heating performances of corn straw particles in a microwave chamber. *Energy Sources Part A Recovery Util. Environ. Eff.* **2023**, *45*, 7186–7197.
35. Santhosh, B.; Ionescu, E.; Andreolli, F.; et al. Effect of pyrolysis temperature on the microstructure and thermal conductivity of polymer-derived monolithic and porous SiC ceramics. *J. Eur. Ceram. Soc.* **2021**, *41*, 1151–1162.
36. Zhang, Z.; Huang, K.; Mao, C.; et al. Microwave assisted catalytic pyrolysis of bagasse to produce hydrogen. *Int. J. Hydrog. Energy* **2022**, *47*, 35626–35634.
37. Fan, Y.; Jin, L.; Ji, W.; et al. Microwave-induced carbonization of rapeseed shell for bio-oil and bio-char: Multi-variable optimization and microwave absorber effect. *Energy Convers. Manag.* **2019**, *191*, 23–38.
38. Reddy, B.R.; Malhotra, A.; Najmi, S.; et al. Microwave assisted heating of plastic waste: Effect of plastic/susceptor (SiC)

contacting patterns. *Chem. Eng. Process.-Process Intensif.* **2022**, *182*, 109202.

39. Fan, L.; Song, H.; Lu, Q.; et al. Screening microwave susceptors for microwave-assisted pyrolysis of lignin: Comparison of product yield and chemical profile. *J. Anal. Appl. Pyrolysis* **2019**, *142*, 104623.